

# Fingerprints of the Magnetic Polaron in Nonequilibrium Electron Transport through a Quantum Wire Coupled to a Ferromagnetic Spin Chain

Frank Reininghaus, Thomas Korb, and Herbert Schoeller  
 Institut für Theoretische Physik A, RWTH Aachen, 52056 Aachen, Germany  
 (Dated: April 14, 2024)

We study nonequilibrium quantum transport through a mesoscopic wire coupled via local exchange to a ferromagnetic spin chain. Using the Keldysh formalism in the self-consistent Born approximation, we identify fingerprints of the magnetic polaron state formed by hybridization of electronic and magnon states. Because of its low decoherence rate, we find coherent transport signals. Both elastic and inelastic peaks of the differential conductance are discussed as a function of external magnetic fields, the polarization of the leads and the electronic level spacing of the wire.

PACS numbers: 73.23.-b, 75.10.Jm, 75.75.+a, 72.25.-b

**Introduction.** In recent years, the field of Spintronics has attracted increasing interest [1, 2]. A considerable amount of theoretical and experimental attention has been focused on transport phenomena, especially spin-dependent charge currents in low-dimensional structures made of magnetic materials [3, 4, 5], but also transport of magnetization through insulating spin chains and quantum dots [6, 7].

In this Letter, we study the interplay between nonequilibrium electron transport and magnetic degrees of freedom in a one-dimensional system. The model under consideration is a finite quantum wire which is coupled via local exchange to a one-dimensional ferromagnetic Heisenberg spin chain and via tunneling to two large electronic reservoirs. Examples of one-dimensional systems which exhibit ferromagnetic coupling of localized spins are so-called "sandwich clusters" formed from vanadium and benzene [8, 9, 10]. Usually, one would expect that emission of magnons in the spin chain will lead to a relaxation and dephasing of the electron spins antiparallel to the spin direction of the spin chain, leading to incoherent transport for this spin direction. However, it was shown in several works on ferromagnetic semiconductors [11, 12, 13, 14] that a single electron with antiparallel spin direction to the localized spins can hybridize with one-magnon states to form the so-called magnetic polaron states. These states form a band which is separated from the band of scattering states, and therefore have a low decoherence rate. The aim of this Letter is to find fingerprints of these states in coherent transport signals at low temperatures by studying the differential conductance as a function of bias voltage. We note that one-electron scattering in finite quantum spin chains has been studied in Ref. [4] at low temperatures with the result of an interesting resonance structure as a function of the Fermi level. However, this work was restricted to linear transport, so that only states near the Fermi level contributed to transport. Therefore, the influence of the magnetic polaron states (lying outside the band of scattering states) was not probed there.

We calculate the differential conductance  $G = \frac{dI}{dV}$  for

large ( $N = 1000$  sites) and small ( $N = 12$  sites) systems which differ in the electronic level spacing. We find peak structures which are due to elastic and inelastic transport processes. The applied magnetic field, the spin polarizations of the leads and the bias voltage affect the energies and decay rates of the electronic states of the system. One can thus control the position and height of the peaks in the differential conductance and identify the processes which contribute to the current.

**Hamiltonian.** We employ a tight-binding model for the quantum wire and a Heisenberg model with ferromagnetic coupling  $J > 0$  for the spin chain (see Fig. 1). They have the same lattice constant  $a$  and Zeeman splittings  $\hbar\omega_e$  and  $E_Z$ , respectively:

$$H_{\text{wire}} = \sum_i t c_i^\dagger c_{i+1} + \text{H.c.} + \frac{1}{2} \hbar\omega_e \sum_i c_i^\dagger c_i$$

$$H_{\text{spin}} = J \sum_i S_i S_{i+1} + E_Z \sum_i S_i^z$$

with  $\hbar = 1$ ,  $\omega_e = \frac{E_Z}{\hbar}$  (we will frequently write  $\omega_e = \omega$  or  $\omega_e = \omega_Z$  instead). We consider low electron densities in the wire and therefore neglect the Coulomb interaction.

We follow [12] and use the Holstein-Primakoff transformation (HPT) [15] to replace the spin operators  $S_i^\pm$  in the chain by boson operators:  $S_i^+ = \sqrt{2S} b_i^\dagger$ ,  $S_i^- = \sqrt{2S} b_i$ ,  $S_i^z = S - b_i^\dagger b_i$ . This approximation is valid if the spin

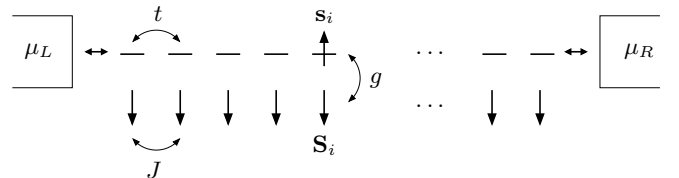


FIG. 1: The model under consideration. The conduction electrons can hop between neighboring sites in the wire, and the localized spins are coupled ferromagnetically. There is a local coupling between the spin of the conduction electrons and the localized spin at each site. The wire is coupled to two leads with the chemical potential  $\mu_L$  and  $\mu_R$ , respectively.

chain is near its ferromagnetic ground state where  $\hbar S_i^z = S$ .

The Zeeman energy  $E_Z$  must be sufficiently large to ensure that this is the case. Using periodic boundary conditions, we can write  $H_{\text{wire}} = \sum_k \epsilon_k c_k^\dagger c_k$ ,  $H_{\text{spin}} = E_0 + \sum_k \epsilon_k^\dagger b_k^\dagger b_k$ , where  $E_0 = -NJS^2 - NSE_Z$  is the ground state energy of the spin chain,  $b_k^\dagger$  and  $b_k$  are creation and annihilation operators for magnons, and  $\epsilon_k = 2t \cos(ka) + \frac{1}{2} \hbar e$ ,  $\epsilon_k^\dagger = 2JS(1 - \cos(ka)) + E_Z$  are one-electron and one-magnon energies, respectively. If  $E_Z \gg JS$ , we can assume that the magnon energies are independent of the wave number:  $\epsilon_k^\dagger = \epsilon_k = E_Z$ .

The interaction  $V = g \sum_i S_i S_i$  between electron spins  $s_i = \frac{1}{2} c_{i\uparrow}^\dagger c_{i\downarrow}$  and localized spins  $S_i$  is transformed using the HPT to  $V = V^{(1)} + V^{(2)} + \dots$ , where

$$V^{(1)} = g \sum_{kq} \frac{S}{2N} \sum_{\alpha\beta} b_{q+\alpha}^\dagger c_{k+\alpha}^\dagger c_{k+\beta} b_{q+\beta}^\dagger c_{k+\beta}^\dagger$$

corresponds to spin flips of a conduction electron which involve the emission or absorption of a magnon,  $V^{(2)} = \frac{g}{2N} \sum_{kq} b_{q+q_0}^\dagger b_{q-q_0}^\dagger c_{k+q_0}^\dagger c_{k+q_0}^\dagger$  in plicates electron-magnon scattering, and  $\epsilon_{q_0}$  is a spin-dependent energy shift which can be combined with  $\epsilon_k$  to form a new one-electron energy  $\epsilon_k = 2t \cos(ka) + \frac{1}{2} (\hbar e - gS)$ .

The wire is coupled to the leads by  $H_T = \sum_{lk} t a_{l1}^\dagger c_k + \text{H.c.}$ . Here,  $2f_L/Rg$  labels the lead and  $l$  the electronic states with energies  $\epsilon_l$ . The leads are assumed to be noninteracting and to have a constant, but possibly spin-dependent, density of states. This is reflected in the energy-independent coupling function  $\Gamma_l(\epsilon) = 2 \sum_l t_l^2 \delta(\epsilon - \epsilon_l)$ .

We assume that the occupation of magnon states is equal to the equilibrium value  $n(\epsilon) = (\exp(\beta \epsilon) + 1)^{-1}$ , i.e., that the coupling to an external spin bath causes magnon relaxation on a time scale  $\tau_M$  which is smaller than the average time between two electron transmissions through the wire but larger than the time needed to establish a coherent electron-magnon state [18].

Method. The nonequilibrium Green function method proposed by Keldysh [16] is used to calculate the current through the wire which can be expressed in terms of the Green functions [17]. We divide the electron self-energy into two parts,  $\Sigma = \Sigma_T + \Sigma_M$ , where  $\Sigma_T$  is due to  $H_T$ . Its retarded/advanced and Keldysh components are  $\Sigma_T^{R,A} = \frac{i}{2}$  and  $\Sigma_T^K(\epsilon) = i(2f(\epsilon) - 1)$ , respectively, where  $\mu = \mu_L$  and  $f(\epsilon)$  is the Fermi function for lead  $L$ , which has the chemical potential  $\mu_L$ .

The self-energy contribution  $\Sigma_M$ , which is due to the electron-magnon interaction  $V$ , is calculated in self-consistent Born approximation (SCBA), which corresponds to the consideration of diagrams of the order  $O(g^2)$ . We evaluate  $\Sigma_M$  using the free magnon Green functions which do not depend on the magnon wave number due to the approximation  $\epsilon_k^\dagger = \epsilon_k$ . Therefore,  $\Sigma_M$  is independent of the electron wave number. With

$M(\epsilon) = \sum_k G_k^R(\epsilon)^2$ , its imaginary part is given by

$$\text{Im} \Sigma_M^R(\epsilon) = \frac{g^2 S}{4N} M(\epsilon) f(\epsilon); \quad (1)$$

where  $f^+ = f$ ,  $f^- = 1 - f$ . The real part is obtained from the Kramers-Kronig relations. Terms which are proportional to  $n(\epsilon)$  have been omitted because  $n(\epsilon) \ll 1$  for the parameters chosen in the next section. Dyson's equation and (1) are solved self-consistently using an iterative procedure [19].

Richmond [12] obtained the exact  $\pi$ -electron self-energy for a single conduction electron in equilibrium by considering a larger set of diagrams involving an arbitrary number of electron-magnon scattering vertices between the emission and absorption vertices. However, these diagrams would give rise to a violation of charge conservation in the nonequilibrium situation which is discussed here (i.e. the sum of the currents from the leads would be nonzero:  $I_L + I_R \neq 0$ ). We therefore restrict our calculation to the charge-conserving SCBA and disregard diagrams of higher order than  $O(g^2)$  [20].

Electrons which tunnel into the system from lead  $L$  with spin  $\uparrow$  can either tunnel to lead  $R$  with unchanged spin (elastic current) or flip their spin by emitting or absorbing a magnon and leave the system with spin  $\downarrow$  (inelastic current). The two current contributions for lead  $L$  are

$$I^{\text{el}} = \frac{e}{h} \int d\epsilon \sum_{\alpha\beta} T_{\alpha\beta}^{\text{el}}(\epsilon) (f_L(\epsilon) - f_R(\epsilon));$$

$$I^{\text{inel}}(\epsilon) = \frac{e}{h} \int d\epsilon \sum_{\alpha\beta} T_{\alpha\beta}^{\text{inel}}(\epsilon; \epsilon') f_L(\epsilon) (1 - f_R(\epsilon'))$$

$$+ T_{\alpha\beta}^{\text{inel}}(\epsilon; \epsilon') (1 - f_L(\epsilon)) f_R(\epsilon');$$

where we have again neglected terms  $\propto n(\epsilon)$ . The transmission coefficients are given by

$$T_{\alpha\beta}^{\text{el}}(\epsilon) = \delta_{\alpha\beta} M(\epsilon); \quad (2)$$

$$T_{\alpha\beta}^{\text{inel}}(\epsilon; \epsilon') = \frac{g^2 S}{2N} \sum_{\gamma\delta} M_{\gamma\delta}(\epsilon) M_{\gamma\delta}(\epsilon'); \quad (3)$$

We consider both nonmagnetic and ferromagnetic leads with polarization  $P = (n_{\uparrow} - n_{\downarrow}) / (n_{\uparrow} + n_{\downarrow}) \neq 0$ .

Results. The differential conductance for a large system with  $N = 1000$  sites where the level spacing is smaller than the other relevant energy scales is shown in Fig. 2. Since the electron density in the wire should be sufficiently low to justify the neglect of the Coulomb interaction, we examine the voltage regime where only a small fraction of the  $\pi$ - and  $\pi$ -electron states is partially occupied. We fix  $\mu_R$  below the conduction band at  $\mu_R = -2.5$  and vary  $\mu_L$  (all energies are in units of  $t$  which we set to  $t = 1$ ).

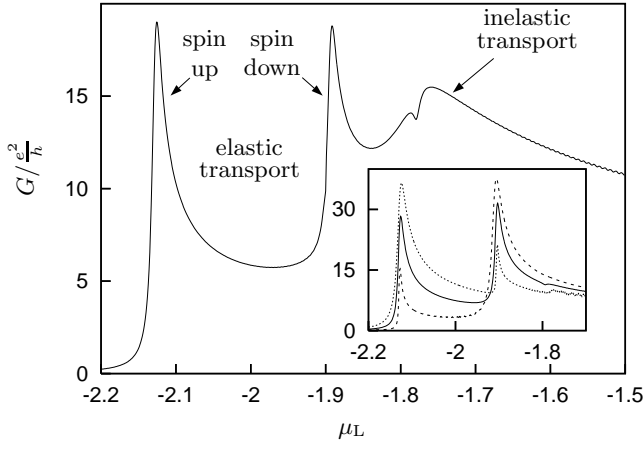


FIG. 2: Differential conductance for a system with  $N = 1000$  sites and  $S = 1/2$ . The parameters are  $t = 1$ ,  $g = 0.5$ ,  $E_Z = h_e = 0.1$ ,  $k_B T = 5 \cdot 10^{-4}$ ,  $\mu_{L,R} = 10^{-2}$ ,  $P_L = +0.7$ ,  $P_R = -0.7$ . The chemical potential  $\mu_R$  of the right lead is fixed at  $-2.5$ . Inset: Conductance for unpolarized leads (solid line) and ferromagnetic leads with parallel polarization and  $P = +0.7$  (dotted line),  $P = -0.7$  (dashed line).

For low bias voltages ( $\mu_L < -1.85$ ), elastic transport processes (corresponding to resonances of  $G_k^R(E)^2$ ) dominate. One peak at  $\mu_L \approx -2.12$  for spin-up is due to the magnetic polaron band, and the other at  $\mu_L \approx -1.89$  corresponds to  $\uparrow$ -electron states. The shape of the peak structures reflects the density of states in a one-dimensional system. Inelastic processes superpose these structures. In the situation where  $P_L = +0.7$  and  $P_R = -0.7$  (main plot of Fig. 2), they dominate for higher voltages ( $\mu_L > -1.85$ ) because this setup maximizes the product  $\mu_L^L \mu_R^R$  which is proportional to the inelastic transmission coefficient (3). The inset of Fig. 2 shows how the different peaks can be distinguished by changing the spin polarization of the leads. Here, three conductance curves are shown for unpolarized leads and ferromagnetic leads with parallel polarizations ( $P_L = P_R = P$ ). The weight of the peak structure which is related to elastic transport of electrons with spin  $\uparrow$  is greatest if the leads are  $\uparrow$ -polarized ( $2f^{\uparrow}/\#g$ ), just as one would expect. While there is also an inelastic current contribution in these configurations, it does not cause a clear signal in the differential conductance.

For a small system with  $N = 12$  sites, the discrete structure of the energy spectrum can be identified in the differential conductance if the level spacing is larger than the energy scales  $\hbar\omega$  and  $k_B T$  which determine the broadening of the conductance peaks. In the considered voltage regime, only the lowest electronic states (wave number  $k = 0$ , spin  $\uparrow$  or  $\downarrow$ ) are partially occupied and contribute to the current. The electronic spin-up states are split mainly by the  $q = 0$  magnon into two states with energy  $\epsilon_{\uparrow}$  and  $\epsilon_{\uparrow}^0$  (corresponding to the magnetic polaron and the scattering state in the continuum case, respec-

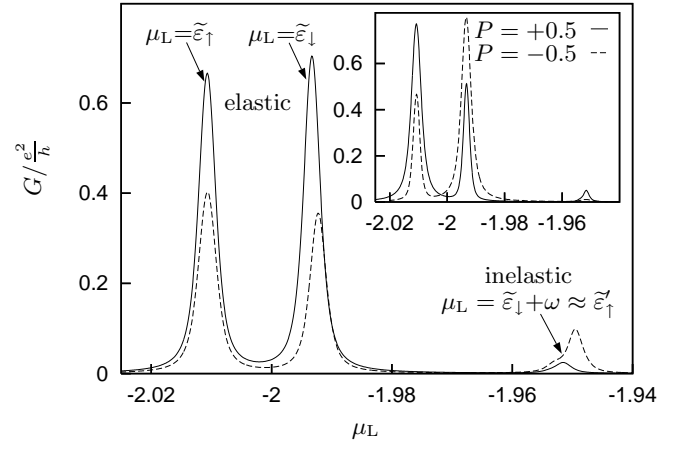


FIG. 3: Conductance for  $N = 12$ ,  $S = 1/2$ . The parameters are  $t = 1$ ,  $g = 0.1$ ,  $E_Z = h_e = 0.04$ ,  $k_B T = 5 \cdot 10^{-4}$ ,  $\mu_{L,R} = 2 \cdot 10^{-3}$ ,  $\mu_R = -2.5$ . Both nonmagnetic leads (solid line) and spin-polarized ferromagnetic leads with  $P_L = +0.7$ ,  $P_R = -0.7$  (dashed line) are considered. Inset:  $G$  for ferromagnetic leads with parallel polarization.

tively). Furthermore, the electronic spin down states are also renormalized to  $\epsilon_{\downarrow}$  when the  $\uparrow$ -electron states have a finite occupation probability.

Results for  $g > 0$  (antiferromagnetic local exchange coupling) are presented in Fig. 3. As in the situation discussed above, conductance peaks which are due to elastic transport processes coincide with resonances of the retarded Green functions. Here, the left and right large peak occur at  $\epsilon_{\uparrow}$  and  $\epsilon_{\downarrow}$ , the main resonances of the  $\uparrow$ - and  $\downarrow$ -electron Green function (with wave number  $k = 0$ ), respectively, and can be attributed to elastic transport through the wire. On the other hand, the inelastic transmission coefficient (3) is proportional to both  $G_k^R(E)^2$  and  $G_{k\#}^R(E - \hbar\omega)^2$ . Therefore, inelastic transport processes contribute to the differential conductance at  $\mu_L = \epsilon_{\uparrow}$  (where some weight is added to the left large peak) and  $\mu_L = \epsilon_{\downarrow} + \hbar\omega$ , the position of the smaller peak. The dependence of the relative peak heights on the lead polarizations is like in the large system discussed above.

Actually, one could expect another peak in Fig. 3 because the  $\uparrow$ -electron Green function has a second resonance at an energy  $\epsilon_{\uparrow}^0$ . However, it has in general quite a small weight because the magnitude of the imaginary part of the  $\uparrow$ -electron self-energy is rather large at  $\epsilon_{\uparrow}^0$ , leading to a strong decay of the corresponding state and a suppression of elastic transport. Moreover,  $\epsilon_{\uparrow}^0$  is very close to the energy  $\epsilon_{\downarrow} + \hbar\omega$  where inelastic transport contributes to the current. Therefore, elastic transport of  $\uparrow$  electrons is visible only at  $\epsilon_{\uparrow}$  (energy of the magnetic polaron), the small contribution at  $\mu_L = \epsilon_{\uparrow}^0$  is absorbed in the inelastic peak.

It should be noted that not only the peak heights but also the positions depend on the polarizations of the leads. Fig. 3 shows that the peak at  $\mu_L = \epsilon_{\downarrow}$  and the

inelastic peak are shifted to the right for the configuration where the leads have antiparallel polarizations. The reason is that a  $\uparrow$  electron (or hole) can interact with magnons only by flipping its spin and occupying an  $\uparrow$  state. Therefore, the  $\uparrow$ -electron self-energy (and thus the position  $\tilde{\epsilon}_\uparrow$  of the main resonance of the Green function) depends on the occupation probability of  $\uparrow$ -electron states. This probability is given by  $F_\uparrow(E) = \frac{1}{2} f(E)$  for a state with energy  $E$  and is affected by both the chemical potentials and the polarizations of the leads.

Conductance curves for ferromagnetic local exchange coupling ( $g < 0$ ) and different magnetic fields are shown in Fig. 4. The Zeeman splitting  $E_z$  of the localized spins is chosen to be twice as large as the splitting  $\hbar_e$  of the conduction electrons. Therefore, not only the peak positions but also the general structure of the conductance curve change if the magnetic field is varied. For small ( $\hbar_e = 0.02$ ) and large ( $\hbar_e = 0.06$ ) fields, the situation is comparable to Fig. 3: There are two large 'elastic' peaks at  $\mu_L = \tilde{\epsilon}_\uparrow$  and  $\mu_L = \tilde{\epsilon}_\downarrow$  and a small 'inelastic' peak at  $\mu_L = \tilde{\epsilon}_\uparrow + 1$ . These peaks move with different 'velocities' if the field is increased: The positions of the large peaks, i.e., of the main resonances of the retarded Green functions, change with the conduction electron Zeeman energy  $\hbar_e/2$ , but the position of the inelastic peak changes like  $\hbar_e/2 + E_z = 3\hbar_e/2$  because of our choice  $E_z = 2\hbar_e$ . One could expect that the inelastic and the right elastic peak overlap and form a single resonance for intermediate fields ( $\hbar_e = 0.045$ ), but this is not the case. The corresponding conductance curve rather reveals two peaks of comparable height. These arise from two resonances of the  $\uparrow$ -electron Green function which have approximately equal weight for this particular set of parameters. This means that the decoherence rates are equal for the states corresponding to the energies  $\tilde{\epsilon}_\uparrow$  and  $\tilde{\epsilon}_\downarrow$ , in contrast to the situation in Fig. 3. Elastic transport of  $\uparrow$  electrons thus generates a double-peak structure in the differential conductance which is superposed by a small inelastic transport contribution.

We remark that without coupling to the spin chain ( $g = 0$ ), there would be only elastic transport through the wire. The effects discussed here, i.e., inelastic transport, a dependence of peak positions on the lead polarization, and magnetic field-dependent decoherence rates of the states involved in transport, would not occur.

**Summary.** We presented a self-consistent diagrammatic approach within the Keldysh formalism to calculate the nonequilibrium current through a mesoscopic quantum wire coupled to a ferromagnetic spin chain. We proposed a way to detect the coherent superposition of electronic and magnon states, the so-called magnetic polaron. It shows up as a high (i.e. coherent) signal in the differential conductance and can be tuned by external magnetic fields and the spin polarization in the leads. In this way we have shown that the interaction between elec-

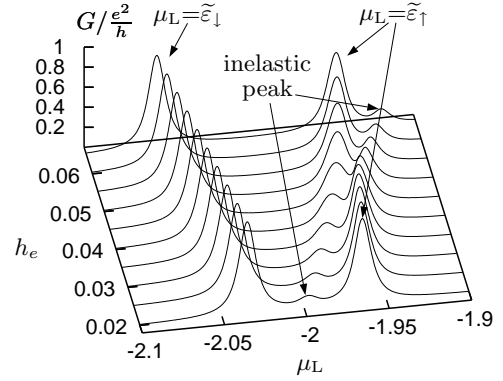


FIG. 4: Conductance for  $t = 1$ ,  $g = -0.1$ ,  $\hbar_e T = 10^{-3}$ ,  $\mu_{L,R} = 5.5 \cdot 10^{-3}$ ,  $\mu_R = 2.5$ . The Zeeman splittings  $\hbar_e$  for conduction electrons and  $E_z = 2\hbar_e$  for localized spins are different for each curve.

trons and magnons (which usually leads to unwanted relaxation and dephasing of the electron spin) can be used for the creation of a phase-coherent quantum state. We expect that this work will stimulate further theoretical and experimental investigations of the magnetic polaron in the field of mesoscopic systems.

The authors would like to thank S. Jakobs and J. König for helpful discussions. This work has been supported by the VW Foundation and the Forschungszentrum Jülich (via the virtual institute IFM II).

- 
- [1] S. A. Wolf et al., *Science* 294, 1488 (2001).
  - [2] I. Zutic, J. Fabian, and S. Das Sarma, *Rev. Mod. Phys.* 76, 323 (2004).
  - [3] V. Rodrigues et al., *Phys. Rev. Lett.* 91, 096801 (2003).
  - [4] Y. A. Vishai and Y. Tokura, *Phys. Rev. Lett.* 87, 197203 (2001).
  - [5] C. Gould et al., (2005), cond-mat/0501597.
  - [6] F. Meier and D. Loss, *Phys. Rev. Lett.* 90, 167204 (2003).
  - [7] O. Strelcyk, T. Körb, and H. Schoeller, *Phys. Rev. B* 72, 165343 (2005).
  - [8] K. Miyajima et al., *J. Am. Chem. Soc.* 126, 13202 (2004).
  - [9] J. Wang, P. H. Acioli, and J. Jellinek, *J. Am. Chem. Soc.* 127, 2812 (2005).
  - [10] H. S. Kang, *J. Phys. Chem. A* 109, 9292 (2005).
  - [11] S. M. Hessel and D. C. Mattis, in *Handbuch der Physik*, edited by S. Flügge (Springer-Verlag, Berlin, 1968), vol. XV III/1, pp. 419-424.
  - [12] P. Richmond, *J. Phys. C* 3, 2402 (1970).
  - [13] B. S. Shastry and D. C. Mattis, *Phys. Rev. B* 24, 5340 (1981).
  - [14] W. Nolting, *Phys. Status Solidi B* 96, 11 (1979).
  - [15] R. Holstein and H. Primakoff, *Phys. Rev.* 58, 1098 (1940).
  - [16] L. V. Keldysh, *Soviet Physics JETP* 20, 1018 (1965).
  - [17] Y. Meir and N. S. Wingreen, *Phys. Rev. Lett.* 68, 2512 (1992).
  - [18] In terms of the energy scales involved,  $\mu_m$  has to fulfill

$\mathcal{J}^{\mu} = \mathcal{J}^{\mu}_{\text{gS}} + \mathcal{J}^{\mu}_1$  to justify this approximation.

[19] We remark that a non-self-consistent solution (which corresponds to stopping the procedure after the first iteration) yields qualitatively different results.

[20] We remark that the problem could be solved if an-

other set of more complex self-energy diagrams was taken into consideration additionally. The discussion of a charge-conserving approximation involving higher-order diagrams will be addressed in a future publication, but does not change the qualitative effects discussed here.